JOURNAL OF THEORETICAL
AND APPLIED MECHANICS
43, 3, pp. 487-500, Warsaw 2005

CONTROLLER DESIGN AND IMPLEMENTATION FOR ACTIVE VIBRATION SUPPRESSION OF A PIEZOELECTRIC SMART SHELL STRUCTURE

Ulrich Gabbert
Tamara Nestorović-Trajkov
Heinz Köppe

Institut für Mechanik, Otto-von-Guericke Universität Magdeburg, Magdeburg, Germany
e-mail: ulrich.gabbert@mb.uni-magdeburg.de; tamara.nestorovic@mb.uni-magdeburg.de; heinz.koeppe@mb.uni-magdeburg.de

The paper is dealing with the model based controller design for a shell structure attached with piezoelectric patches as actuators and sensors. The state-space model used for the controller design was obtained using the finite element (FE) approach, modal analysis and modal reduction resulting in a form convenient for the controller development. The optimal LQ controller was designed for the vibration suppression purposes of a funnel shaped shell structure. The design model for the controller development was augmented with additional dynamics which takes into account excitations/disturbances, contributing thus to a better vibration suppression. The controller was implemented on a funnel-shaped piezoelectric structure. The structure was intensively investigated experimentally, and the achieved results of the controlled behaviour with respect to vibration suppression are presented and discussed.

Key words: active vibration suppression, optimal controller design, piezoelectric smart structure

1. Introduction

The vibration suppression task represents an important issue, especially in smart structures, which demand active adaptation of the structural behaviour in accordance with environmental conditions. The controller design and its implementation play an important role in achieving this task. In this paper, the controller design for a piezoelectric shell structure is presented as well as its implementation for the vibration suppression of the structure under investigation. For the model based controller design approach, a state-space model of a piezoelectric structure can be developed using the FE analysis, which represents a convenient technique, especially in early phases of the structure development, controller design and simulation verification. This approach was employed in this paper for obtaining a model of the piezoelectric structure.

Piezoelectric sensing and control have been addressed in different papers (e.g. Gabbert and Tzou, 2001; Rao and Sunar, 1993; Tzou and Tseng, 1990; etc.). This paper concerns vibration control of a shell structure using distributed piezoelectric actuator/sensor patches and optimal LQ tracking with additional dynamics implemented as a part of the overall design procedure of smart structures.

In the first part of the paper, the model development using the FE approach is explained, resulting in a state space representation convenient for the controller design. The model based controller design is presented subsequently, combining the optimal LQ controller with an augmented design model which takes into account the influence of periodic excitations in the frequency range of interest, contributing thus to a better vibration suppression. The controller was implemented and tested on a funnel-shaped shell structure attached with piezoelectric actuators and sensors. Experimental results were obtained applying Hardware-in-the-Loop simulation. Finally, the influence of the actuator/sensor placement was also considered and illustrated with an example.

1.1. Finite element based development of a state space model for piezoelectric structures

The approach is based on the development of equations of motion for a piezoelectric structure approximated by a given number of finite elements. A semi-discrete form of the equations of motion of the finite element can be derived using an approximation method of displacements and electric potential (Berger *et al.*, 2000; Gabbert, 2002; Görnandt and Gabbert, 2002). That approach was used to develop a comprehensive library of multi-field finite elements (1D, 2D, 3D elements, thick and thin layered composite shell elements etc.), which was implemented in our finite element package COSAR (see: http://www.femcos.de). For simulation of thin lightweight structures, curved multi-layer shell elements developed on the basis of the classical *Semi-Loof* element family (Irons, 1976) have proved to give good results. Following the Kirchhoff-Love hypothesis, three different approaches were developed to include fully coupled electro-mechanical behaviour into the SemiLoof elements (Gabbert *et al.*, 2002; Seeger *et al.*, 2002). The material properties of an active fibre composite can be calculated by applying a homogenisation procedure (Berger *et al.*, 2003).

As a result of the FE analysis, behaviour of a structure approximated by an arbitrary number of finite elements can be described with assembled equations of motion in a semi-discrete form (Gabbert *et al.*, 2002; Nestorović-Trajkov *et al.*, 2003a)

$$\mathbf{M}\ddot{\boldsymbol{q}} + \mathbf{D}_d\dot{\boldsymbol{q}} + \mathbf{K}\boldsymbol{q} = \overline{\boldsymbol{F}} \tag{1.1}$$

where $\mathbf{M}$, $\mathbf{D}_d$ and $\mathbf{K}$ are the mass matrix, the damping matrix and the stiffness matrix, respectively, and vector $\boldsymbol{q}$ represents the vector of generalized displacements (including mechanical displacements and electric potential), and contains all degrees of freedom. The total load vector $\overline{\boldsymbol{F}}$ is divided into the vector of external forces $\boldsymbol{F}_E$ and the vector of control forces $\boldsymbol{F}_C$

$$\overline{\boldsymbol{F}} = \boldsymbol{F}_E + \boldsymbol{F}_C = \overline{\mathbf{E}}\boldsymbol{w}(t) + \overline{\mathbf{B}}\boldsymbol{u}(t) \tag{1.2}$$

where the forces are generalized quantities including also electric charges. The vector $\boldsymbol{w}(t)$ represents the vector of external disturbances and $\boldsymbol{u}(t)$ is the vector of the controller influence on the structure. The matrices $\overline{\mathbf{E}}$ and $\overline{\mathbf{B}}$ describe the positions of forces and control parameters in the finite element structure, respectively. As a convenient procedure for obtaining the state space model, modal truncation is adopted since the high order of the FE model represented by equation (1.1) is not suitable for the controller design and the reduction of the model order is required. A decoupled system of equations (1.3) in modal coordinates $\boldsymbol{z}$ is obtained by performing ortho-normalization with $\boldsymbol{\Phi}_m^\top\mathbf{M}\boldsymbol{\Phi}_m = \mathbf{I}$ and $\boldsymbol{\Phi}_m^\top\mathbf{K}\boldsymbol{\Phi}_m = \boldsymbol{\Omega}$, where the modal matrix $\boldsymbol{\Phi}_m$ and the spectral matrix $\boldsymbol{\Omega}$ are obtained from the solution to the linear eigenvalue problem for (1.1). In the decoupled system of equations

$$\ddot{\boldsymbol{z}} + \boldsymbol{\Delta}\dot{\boldsymbol{z}} + \boldsymbol{\Omega}\boldsymbol{z} = \boldsymbol{\Phi}_m^\top\overline{\boldsymbol{F}} \tag{1.3}$$

the matrix $\boldsymbol{\Delta} = \boldsymbol{\Phi}_m^\top\mathbf{D}_d\boldsymbol{\Phi}_m$ represents the modal damping matrix. Generalised displacements $\boldsymbol{q}$ are related to modal coordinates $\boldsymbol{z}$ by

$$\boldsymbol{q}(t) = \boldsymbol{\Phi}_m\boldsymbol{z}(t) \tag{1.4}$$

In the modal truncation procedure, the modal displacement vector $\boldsymbol{z}$ is partitioned and only a part $\boldsymbol{z}_r$ corresponding to selected eigenmodes of interest for the control is retained. Introducing the modal reduced state vector

$$\boldsymbol{x}(t) = \begin{bmatrix} \boldsymbol{z}_r(t) \\ \dot{\boldsymbol{z}}_r(t) \end{bmatrix} \tag{1.5}$$

the modal reduced model is obtained in the state space form

$$\dot{\boldsymbol{x}} = \begin{bmatrix} \mathbf{0} & \boldsymbol{I} \\ -\boldsymbol{\Omega}_r & -\boldsymbol{\Delta}_r \end{bmatrix} \boldsymbol{x} + \begin{bmatrix} \mathbf{0} \\ \boldsymbol{\Phi}_r^\top \overline{\mathbf{B}} \end{bmatrix} \boldsymbol{u}(t) + \begin{bmatrix} \mathbf{0} \\ \boldsymbol{\Phi}_r^\top \overline{\mathbf{E}} \end{bmatrix} \boldsymbol{w}(t) \tag{1.6}$$

where the matrices $\boldsymbol{\Omega}_r$, $\boldsymbol{\Delta}_r$ and $\boldsymbol{\Phi}_r$ are obtained from an appropriate partition of the matrices $\boldsymbol{\Omega}$, $\boldsymbol{\Delta}$ and $\boldsymbol{\Phi}_m$, respectively. Written in a standard state space form, the state equation of the model becomes

$$\dot{\boldsymbol{x}}(t) = \mathbf{A}\boldsymbol{x}(t) + \mathbf{B}\boldsymbol{u}(t) + \mathbf{E}\boldsymbol{w}(t) \tag{1.7}$$

Using a similar procedure, a state space formulation of the output equation is obtained

$$\boldsymbol{y} = \mathbf{C}\boldsymbol{x}(t) + \mathbf{D}\boldsymbol{u}(t) + \mathbf{F}\boldsymbol{w}(t) \tag{1.8}$$

which assumes, in a general case, the influence of the control and external inputs on the outputs.

2. Controller design

A state-space model of the controlled plant, obtained from the finite element analysis and modal reduction, can be used for the controller design. The model in the form of equations (1.7), (1.8) represents a starting point for the controller design where, in a general case, the presence of the disturbance vector $\boldsymbol{w}$ in the state and output equations is assumed. The optimal LQ control law based on the tracking system design with additional dynamics (Nestorović-Trajkov *et al.*, 2003b; Vacarro, 1995) can be viewed as a successful means for the vibration suppression in smart structures.

The controller design assumes rejection of disturbances/excitations, which cause vibrations, providing thus the controlled system outputs with asymptotically reduced oscillation magnitudes.

The discrete-time state space equivalent of the state space model developed through the FEM procedure and modal reduction is used for the controller design

$$\begin{aligned} \boldsymbol{x}[k+1] &= \boldsymbol{\Phi}\boldsymbol{x}[k] + \boldsymbol{\Gamma}\boldsymbol{u}[k] + \boldsymbol{\varepsilon}\boldsymbol{w}[k] \\ \boldsymbol{y}[k] &= \mathbf{C}\boldsymbol{x}[k] + \mathbf{D}\boldsymbol{u}[k] + \mathbf{F}\boldsymbol{w}[k] \end{aligned} \tag{2.1}$$

where

$$\mathbf{\Phi} = \mathrm{e}^{\mathbf{A}T} \qquad \mathbf{\Gamma} = \int\limits_0^T \mathrm{e}^{\mathbf{A}\tau}\mathbf{B}\, d\tau \qquad \boldsymbol{\varepsilon} = \int\limits_0^T \mathrm{e}^{\mathbf{A}\tau}\mathbf{E}\, d\tau \tag{2.2}$$

and T is the sampling time.

The controller design includes available *a priori* knowledge about the occurring disturbance type contained in the additional dynamics, which represents an important part of the controller design procedure. The additional dynamics is introduced in order to compensate for the presence of the disturbance providing at the same time the tracking of the reference trajectories described by models with the same poles as those of disturbances. Such a controller with the additional dynamics serves for controlling purposes if the reference input to be tracked and the disturbance acting upon the structure can be described by a rational discrete function. This condition is fulfilled by a sine function used as a disturbance model. A special interest in investigation of this type of disturbances has arisen from the fact that periodic disturbances with frequencies corresponding to eigenfrequencies of a smart structure can cause resonance. Taking it into account, this type of disturbance can be considered the worst study case.

The additional dynamics is formed from the coefficients of the polynomial

$$\delta(z) = \prod_i (z - \mathrm{e}^{\lambda_i T})^{m_i} = z^s + \delta_1 z^{s-1} + \ldots + \delta_s \tag{2.3}$$

where λ_i are the poles of the reference input and/or excitation/disturbance. A state space realization of the additional dynamics is expressed in the form of matrices

$$\mathbf{\Phi}_a = \begin{bmatrix} -\delta_1 & 1 & 0 & \cdots & 0 \\ -\delta_2 & 0 & 1 & \cdots & 0 \\ \vdots & \vdots & \vdots & \ddots & \vdots \\ -\delta_{s-1} & 0 & 0 & \cdots & 1 \\ -\delta_s & 0 & 0 & \cdots & 0 \end{bmatrix} \mathbf{\Gamma}_a = \begin{bmatrix} -\delta_1 \\ -\delta_2 \\ \vdots \\ -\delta_{s-1} \\ -\delta_s \end{bmatrix} \tag{2.4}$$

In the case of multiple-input multiple-output (MIMO) systems, the additional dynamics must be replicated in q parallel systems (once per each output), where q is the number of outputs.

The replicated additional dynamics is described by

$$\overline{\mathbf{\Phi}} \stackrel{def}{=} \operatorname{diag}(\underbrace{\mathbf{\Phi}_a, \ldots, \mathbf{\Phi}_a}_{q \text{ times}}) \qquad \overline{\mathbf{\Gamma}} \stackrel{def}{=} \operatorname{diag}(\underbrace{\mathbf{\Gamma}_a, \ldots, \mathbf{\Gamma}_a}_{q \text{ times}}) \tag{2.5}$$

The discrete-time design model $(\mathbf{\Phi}_d, \mathbf{\Gamma}_d)$ is formed as a cascade combination of the additional dynamics $(\mathbf{\Phi}_a, \mathbf{\Gamma}_a)$ or $(\overline{\mathbf{\Phi}}, \overline{\mathbf{\Gamma}})$ and the discrete-time plant model $(\mathbf{\Phi}, \mathbf{\Gamma})$

$$\boldsymbol{x}_d[k+1] = \mathbf{\Phi}_d \boldsymbol{x}_d[k] + \mathbf{\Gamma}_d \boldsymbol{u}[k] \tag{2.6}$$

where

$$\mathbf{\Phi}_d = \begin{bmatrix} \mathbf{\Phi} & \mathbf{0} \\ \mathbf{\Gamma}^* \mathbf{C} & \mathbf{\Phi}^* \end{bmatrix} \qquad \mathbf{\Gamma}_d = \begin{bmatrix} \mathbf{\Gamma} \\ \mathbf{0} \end{bmatrix} \qquad \boldsymbol{x}_d = \begin{bmatrix} \boldsymbol{x}[k] \\ \boldsymbol{x}_a[k] \end{bmatrix} \tag{2.7}$$

and $\mathbf{\Phi}^*$ denotes $\mathbf{\Phi}_a$ or $\overline{\mathbf{\Phi}}$, and $\mathbf{\Gamma}^*$ represents $\mathbf{\Gamma}_a$ or $\overline{\mathbf{\Gamma}}$, depending on whether the controlled structure is modelled as a single-input single-output or a multiple-input multiple-output system, respectively. The gain matrix $\mathbf{L}$ of the optimal LQ regulator is calculated on the basis of the design model (2.6) in such a way that the feedback law $\boldsymbol{u}[k] = -\mathbf{L}\boldsymbol{x}_d[k]$ minimizes performance index (2.8) subject to constraint (20), where $\mathbf{Q}$ and $\mathbf{R}$ are symmetric, positive-definite matrices

$$J = \frac{1}{2} \sum_{k=0}^{\infty} \Big(\boldsymbol{x}_d^\top[k] \mathbf{Q} \boldsymbol{x}_d[k] + \boldsymbol{u}^\top[k] \mathbf{R} \boldsymbol{u}[k] \Big) \tag{2.8}$$

The control system is designed for the realization $(\mathbf{\Phi}_d, \mathbf{\Gamma}_d)$. The feedback gain matrix $\mathbf{L}$ in the control law is partitioned into submatrices $\mathbf{L}_1$ and $\mathbf{L}_2$ formed from the first n and last $q \times s$ columns of the matrix $\mathbf{L}$, respectively

$$\mathbf{L} = \begin{bmatrix} \mathbf{L}_1 & \mathbf{L}_2 \end{bmatrix} \tag{2.9}$$

Thus the feedback gain matrix $\mathbf{L}_1$ corresponds to the state variables of the controlled structure, while the feedback gain matrix $\mathbf{L}_2$ pertains to the rest of the state variables in the design state vector $\boldsymbol{x}_d$ introduced by the additional dynamics.

The design of the controller involves the estimation of the state variables. In the state space model obtained using the FE approach, the state variables are modal variables which are not measurable and their estimation is therefore necessary. For the estimation of the state variables, a Kalman filter can be used. Given the covariances $\mathbf{Q}_w$ and $\mathbf{R}_v$ of the process and measurement noise respectively, the Kalman estimator is defined with the following equations

$$\begin{aligned} \widehat{\boldsymbol{x}}[k] &= \overline{\boldsymbol{x}}[k] + \mathbf{L}_{est}[k](\boldsymbol{y}[k] - \mathbf{C}\overline{\boldsymbol{x}}[k]) \\ \overline{\boldsymbol{x}}[k] &= \mathbf{\Phi}\widehat{\boldsymbol{x}}[k-1] + \mathbf{\Gamma}\boldsymbol{u}[k-1] \end{aligned} \tag{2.10}$$

where the Kalman gain matrix is

$$\mathbf{L}_{est}[k] = \mathbf{P}[k]\mathbf{C}^\top\mathbf{R}_v^{-1} \tag{2.11}$$

and

$$\begin{aligned} \mathbf{P}[k] &= \mathbf{M}_k[k] - \mathbf{M}_k[k]\mathbf{C}^\top(\mathbf{C}\mathbf{M}_k[k]\mathbf{C}^\top + \mathbf{R}_v)^{-1}\mathbf{C}\mathbf{M}_k[k] \\ \mathbf{M}_k[k+1] &= \boldsymbol{\Phi}\mathbf{P}[k]\boldsymbol{\Phi}^\top + \boldsymbol{\varepsilon}\mathbf{Q}_w\boldsymbol{\varepsilon}^\top \end{aligned} \tag{2.12}$$

The matrices $\mathbf{P}$ and $\mathbf{M}_k$ are determined by solving equations (2.12).

The optimal LQ tracking control system with the additional dynamics and Kalman's estimator is implemented as shown in Fig. 1.

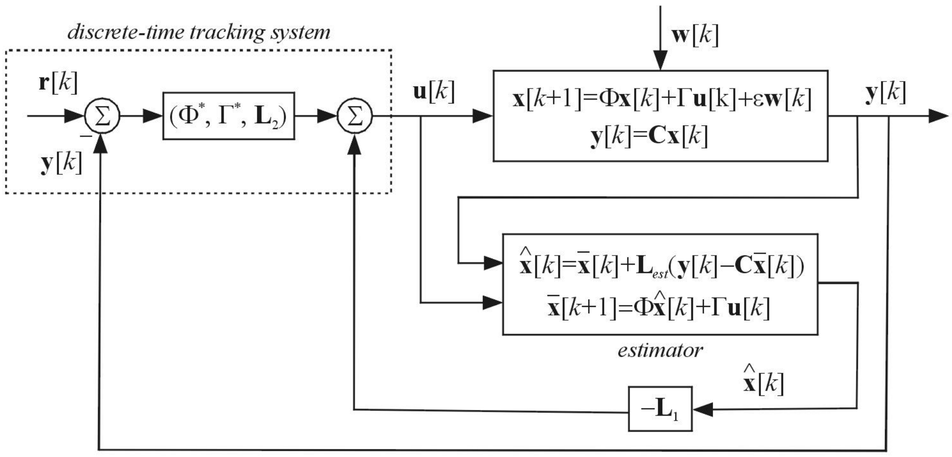

Fig. 1. The optimal LQ tracking system with additional dynamics and a state estimator

3. Implementation in a funnel-shaped structure

Active vibration control using the described controller design and model development procedure was implemented for the vibration suppression of a funnel-shaped shell structure shown in Fig. 2. The funnel is the inlet part of a magnetic resonance image (MRI) tomograph (Fig. 3) used in medical diagnostics.

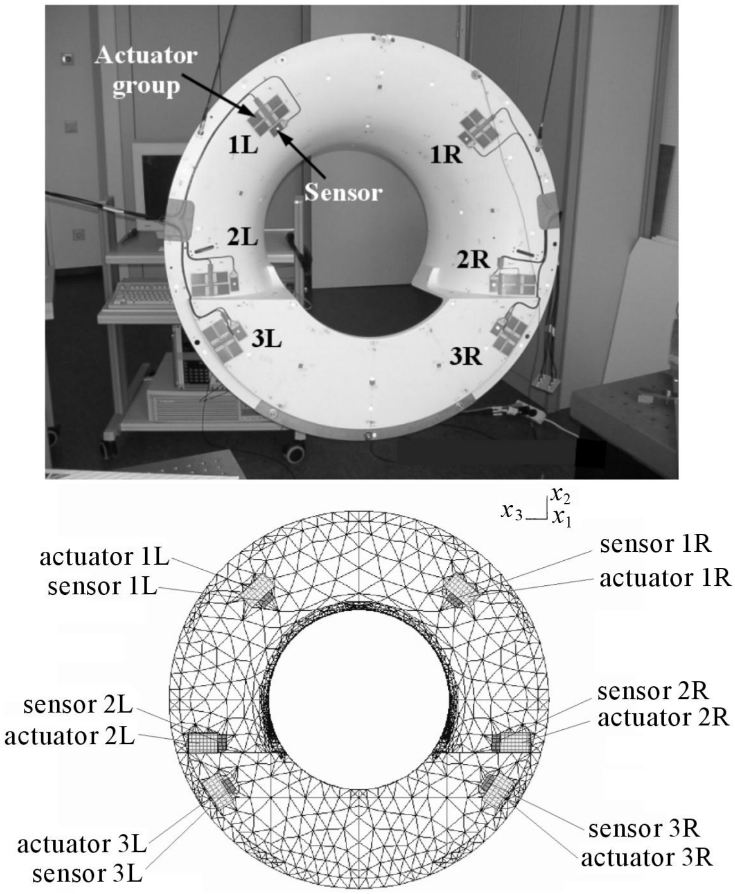

Fig. 2. (a) The funnel of an MRI tomograph with actuator/sensor placement, (b) the finite element mesh of the funnel

Six actuator-groups and six sensors attached to the surface of the funnel are used for experimental modal analysis and vibration control of the structure. They are denoted as 1L, 2L, 3L for the left-hand side actuators and sensors and 1R, 2R, 3R for the right-hand side ones. Each of six actuators represents a group consisting of four piezoelectric patches (function modules). Each of six sensors is a single piezoelectric patch. The function modules are made of piezoceramic films (PZT film Sonox P53) with standard dimensions $50 \times 25 \times 0.2$ [mm]. Applying the FEM-based approach for the analysis of the funnel behaviour and numeric model development (using the finite element software COSAR), the eigenfrequencies were determined and, on the basis of the comparison with experimental results, a reduced order state space model of the funnel was adopted for the control of the funnel eigenmodes in the frequency

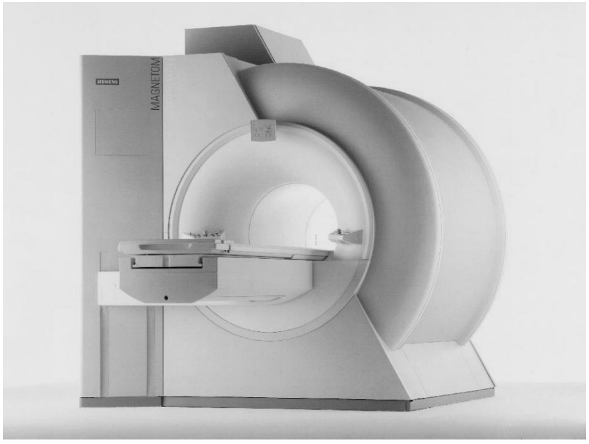

Fig. 3. An MRI tomograph

range up to 35 Hz, where the eigenfrequencies of interest are: $f_1 = 9.573$ Hz, $f_2 = 23.333$ Hz, $f_3 = 31.439$ Hz. As the worst study case of the controller design (with respect to resonance), the excitations brought to the funnel using the shaker are selected as sine signals with frequencies corresponding to the eigenfrequencies of the funnel. The experimental rig for the implementation of the designed optimal LQ controller with the additional dynamics, including the funnel as a part of the Hardware-in-the-Loop (HiL) system is represented in Fig. 4.

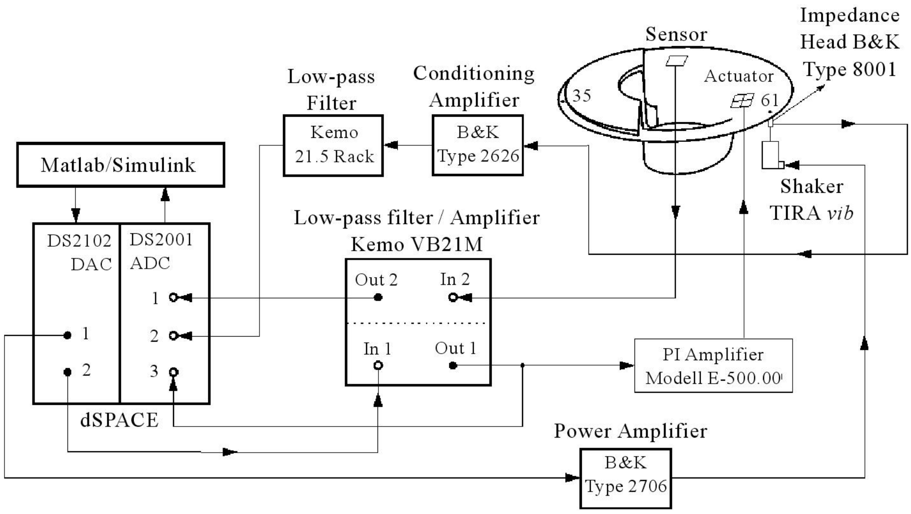

Fig. 4. The funnel of the MRI tomograph within the HiL system with dSPACE

Assuming the sine excitation with the frequency f_1, the control system was designed with the controller parameters $\mathbf{Q} = \mathbf{I}_{8\times 8}$ and $R = 10$. The time response of the sensor S1R and the control effort of the actuator A2R obtained experimentally with this control system in the presence of the sine excitation with the frequency f_1 is shown in Fig. 5. The period without control is clearly indicated by the zero control input and obviously greater vibration magnitudes of the sensor response.

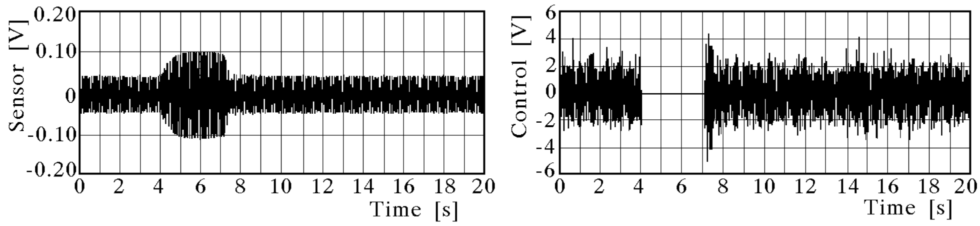

Fig. 5. The response of sensor S1R and control (actuator A2R) in the presence of the sine excitation with the frequency f_1

In the presence of the excitation obtained as a sum of the sinusoids with frequencies f_1, f_2, f_3, the designed controller exhibits behaviour as shown in Fig. 6.

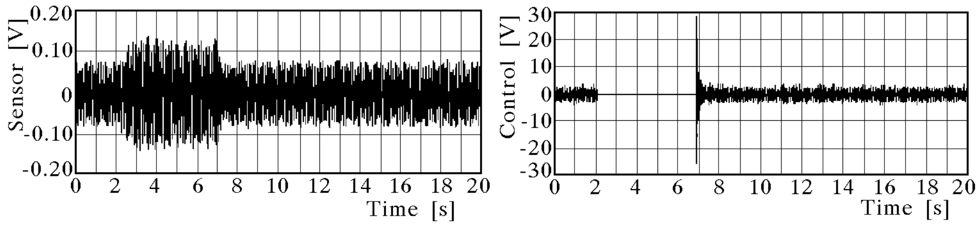

Fig. 6. The sensor response and control with an excitation containing three eigenfrequencies (the control system designed to control the first eigenfrequency)

With the excitation obtained as a sum of the sinusoids with frequencies f_1, f_2, f_3, the control system is designed with the order of the design model 12 and the weighting matrices $\mathbf{Q} = \mathbf{I}_{12\times 12}$ and $R = 10$. This control system performs better vibration suppression (Fig. 7) in comparison with Fig. 6 using a slightly greater control effort.

The influence of the acutator/sensor placement is shown through the comparison of the results for acutaror/sensor pairs A2R−S1R and A2R−S2L (Fig. 8 and Fig. 9). According to the criterion of the overlapped deformation, distributions for the first five eigenmodes of the funnel, regions of ac-

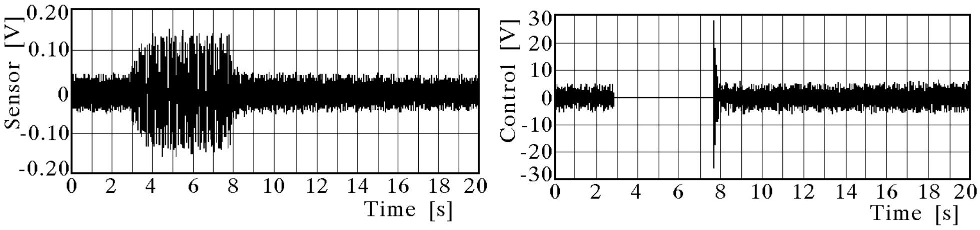

Fig. 7. The sensor signal and control with an excitation containing three eigenfrequencies (the controller designed for simultaneous control of the first three eigenfrequencies)

tuator/sensor position 2L, 2R are determined as the best regions for the actuator/sensor placement. The results shown in Fig. 8 and Fig. 9 confirm this optimal actuator/sensor placement. Actuator/sensor pair A2R – S2L gives better vibration suppression results: in the controlled case the vibration amplitudes are reduced to approximately 7% of the uncontrolled amplitudes (Fig. 9), while with actuator/sensor pair A2R – S1R this reduction reaches approximately 60% of the uncontrolled amplitudes (Fig. 8).

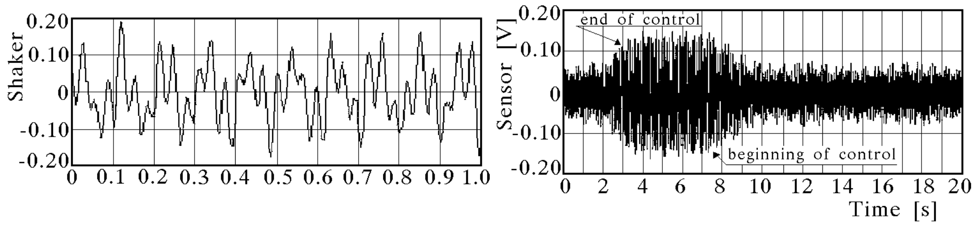

Fig. 8. Actuator/sensor pair A2R – S1R: the excitation obtained as a sum of three sinusoidal signals and response of the sensor in the presence of this excitation

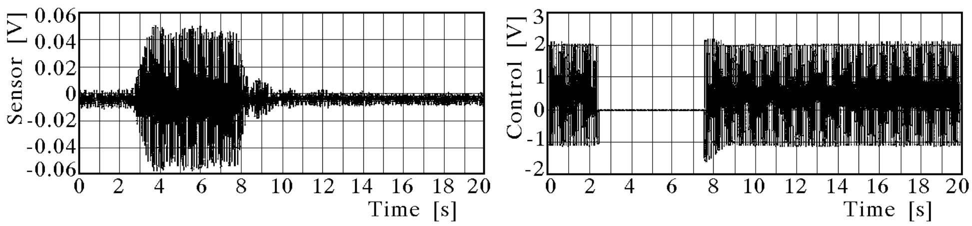

Fig. 9. Actuator/sensor pair A2R – S2L: sensor response and control with an excitation containing three eigenfrequencies

The presented results show efficiency of the control system applied for the reduction of the vibration amplitude. According to expectations, the control system designed taking into account three different frequencies of the periodic excitation exhibits better behaviour in the presence of excitations obtained as a sum of three sinusoidal signals than the controller which takes into account only one eigenfrequency in the presence of the same excitation.

4. Conclusion

In this paper, the model based controller design as a part of the overall design procedure for the development of piezoelectric smart structures is presented. The state space model used as the starting point for the controller design is obtained using the FE approach and modal analysis resulting after appropriate modal reduction in a form convenient for the optimal LQ controller design.

The innovation in the optimal LQ controller design is achieved by introducing additional dynamics to the formulation of the design model for the controller design and connecting the two approaches in order to achieve better controlled performance of the closed-loop system with respect to vibration suppression in the presence of considered excitations. The influence of periodic excitations/disturbances taken into account through the additional dynamics is considered the worst study case due to the possibility of the resonance. The suppression of vibrations caused by such excitations and disturbances represents therefore an important task which was, in this case, demonstrated to be successfully accomplished by applying the control system to the considered funnel shaped piezoelectric shell structure.

Acknowledgement

This work has been partially supported by a postgraduate program of the German Federal State of Saxony-Anhalt. It was motivated and supported by cooperation with the Siemens company in the frame of the German industrial Research project 'Adaptronik' supported by the German Ministry for Education and Research. These supports are gratefully acknowledged.

References

1. BERGER H., GABBERT U., KÖPPE H., RODRIGUEZ-RAMOS R., BRAVO-CASTILLERO J., GUINOVART-DIAZ R., OTERO J.A., MAUGIN G.A., 2003, Finite element and asymptotic homogenization methods applied to smart composite materials, *Journal of Computational Mechanics*, **33**, 61-67

2. Berger H., Gabbert U., Köppe H., Seeger F., 2000, Finite element analysis and design of piezoelectric controlled smart structures, *Journal of Theoretical and Applied Mechanics*, **38**, 3, 475-498

3. Gabbert U., 2002, Research activities in smart materials and structures and expectations to future developments, *Journal of Theoretical and Applied Mechanics*, **40**, 3, 549-574

4. Gabbert U., Köppe H., Seeger F., Berger H., 2002, Modeling of smart composite shell structures. *Journal of Theoretical and Applied Mechanics*, **40**, 3, 575-593

5. Gabbert U., Tzou H.S., 2001, *Smart Structures and Structronic Systems*, Dordrecht Kluwer Academic Publishers

6. Görnandt A., Gabbert U., 2002, Finite element analysis of thermopiezoelectric smart structures, *Acta Mechanica*, **154**, 129-140

7. Irons B.M., 1976, *The Semiloof shell element, in Ashwell DG, Gallagher RH. (Eds.): Finite Elements for Thin Shells and Curved Members*, J. Wiley, London

8. Nestorović-Trajkov T., Gabbert U., Köppe H., 2003a, Controller design for a funnel-shaped smart shell structure, *Facta Universitatis, Series mechanics, automatic control and robotics, Special issue: Nonlinear Mechanic, Nonlinear Sciences and Applications II*, **3**, 15, 1033-1038

9. Nestorović-Trajkov T., Gabbert U., Köppe H., 2003b, Vibration control of a plate structure using optimal tracking based on LQ controller and additional dynamics, *Proceedings of the 3rd World Conference on Structural Control*, 7-12 April 2002, Como, Italy (Vol. 3), editor Fabio Casciati, John Willey & Sons, Ltd., 85-90

10. Rao S.S., Sunar M., 1993, Analysis of distributed thermopiezoelectric sensors and actuators in advanced intelligent structures, *AIAA Journal*, **31**, 7, 1280-1286

11. Seeger F., Gabbert U., Köppe H., Fuchs K., 2002, Analysis and design of thin-walled smart structures in industrial applications, *SPIE Proceedings*, **4698**, 342-350

12. Tzou H.S., Tseng C.I., 1990, Distributed piezoelectric sensor/actuator design for dynamic measurement/control of distributed parameter system: a piezoelectric finite element approach, *J. Sound Vib.*, **138**, 1, 17-34

13. Vaccaro R.J., 1995, *Digital Control: A State-Space Approach*, McGraw-Hill, Inc.

Projektowanie i implementacja sterownika do aktywnej redukcji drgań powłokowej struktury "inteligentnej" z elementami piezoelektrycznymi

Streszczenie

Praca dotyczy problemu modelowego projektowania struktury powłokowej z naklejonymi do niej elementami piezoelektrycznymi. Zastosowany w procesie projektowania model, który opisano w przestrzeni stanu, został sformułowany za pomocą metody elementów skończonych, analizy modalnej i modalnej redukcji, co dało wygodny do implementacji rezultat. Optymalny sterownik LQ zaprojektowano w celu ograniczenia amplitudy drgań struktury powłokowej o lejkowatym kształcie. Użyty model został uzupełniony o zjawiska dynamiczne uwzględniające zewnętrzne wymuszenia i zakłócenia oddziaływujące na powłokę, co poprawiło docelową efektywność aktywnego tłumienia drgań. Ostatecznie, dokonano praktycznego wdrożenia sterownika, który współpracował z lejkowato-kształtną powłoką wyposażną w piezoelektryczne czujniki i elementy wykonawcze. Powłokowa struktura została następnie poddana badaniom eksperymentalnym, a rezultaty pomiarów w kontekście skuteczności redukcji drgań uzyskanej wskutek implementacji analizowanego sterownika zaprezentowano i omówiono w pracy.

Manuscript received December 6, 2004; accepted for print February 8, 2005